Diffusing Light Photography of Fully Developed Isotropic Ripple Turbulence

William B. Wright, Raffi Budakian, and Seth J. Putterman
Physics Department, University of California, Los Angeles, California 90095
(Received 6 February 1996)

The instantaneous height of the entire surface of a fluid executing high amplitude motion can be obtained by photographing light that has been forced to diffuse *through* the liquid. This technique has been applied to resolve solitons and observe the frequency and wave-number spectra of ripple turbulence. Higher order correlations and various models of turbulence can be probed with this method. [S0031-9007(96)00368-7]

PACS numbers: 47.27.Gs, 47.20.Ky

An abiding goal of the physics of continuum mechanics is to understand the fate of energy which is injected into a system so as to drive it far from equilibrium. Prior to its dissipation into heat the energy throughput experiences a competition between randomization and structure formation which in the limit of high amplitude is the problem of turbulence. Capillary waves which propagate on the surface of a fluid make these issues accessible to experimental investigation with a table-top apparatus. At low levels of excitation structural symmetries akin to crystals with dislocations [1], quasicrystals and quantum scars [2] can be seen. Here we report a new imaging technique which makes it possible to simultaneously measure at over 10^6 points the position of a fluid surface whose variations in height are so large that the spectrum of ripple motion is fully developed wave turbulence. For vortex turbulence [3,4] this limit has been demonstrated in nature [5] while laboratory work even at major facilities [6] has been limited to measurements at a couple of points. The accessibility of capillary wave turbulence to controlled laboratory measurements makes it possible to probe not only the power spectrum but also the transition to turbulence, the "Stosszahl ansatz," motion on ultralong time scales and collective modes of turbulence. These correlations probe the foundations of our understanding of turbulence and lie beyond the range of various dimensional and kinetic theories of vortex and wave turbulence [3,4,7–12].

For capillary waves knowledge of the surface height ζ as a function of position $\vec{r}$ and time t uniquely characterizes the motion. In order to quantitatively measure $\zeta(\vec{r}, t)$ for high amplitude motion we suspend in the water 0.04% concentration of polystyrene spheres [13,14] whose diameter ($1\,\mu$m) maximizes the scattering of visible light. The concentration is small enough so as not to affect the viscosity [15] but large enough so that light is scattered so strongly that it diffuses *through* the water [16]. Figure 1 displays a rendering of the surface when a cell containing the fluid ($16.5 \times 19 \times 3$ cm deep) is parametrically excited by vibration (at 50 Hz) perpendicular to the free surface at low and high amplitudes.

To obtain the photos from which Fig. 1 is constructed a flashlamp is used to illuminate the transparent bottom of the cell for 6 μsec. The light then diffuses through the water to the top surface where it is photographed with a Princeton Instruments charge coupled device (CCD) camera (1024×1024 pixels) with 16 bits of dynamic range (65 000 gray scales) focused on the surface with a lens. To minimize photon shot noise the signal was binned into 512×512 superpixels. The exiting intensity is inversely proportional to the local depth so that darker regions are higher ($\zeta > 0$) and the lighter regions are lower than the undisturbed surface height ($\zeta = 0$).

Quantitative information about the surface is obtained by calibrating the transmission of light as a function of fluid depth [17]. For the CCD, experimental parameters can be adjusted so that the change in intensity with depth is 1500 gray scales per mm (the sensitivity is 6 electrons per gray scale which are recorded with a quantum efficiency of 80%) and is linear within 10% over the measured range of heights. Deviations from linearity are corrected for, pixel by pixel.

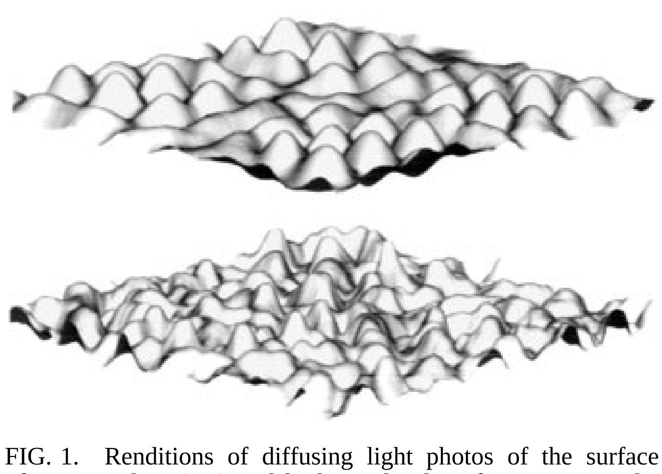

FIG. 1. Renditions of diffusing light photos of the surface of water at low (top) and high amplitudes of excitation. The photos record light that diffuses *through* the fluid, in contrast with shadowgraphs which image the arrival of light fronts (and caustics) on a diffusing plate above the system being probed. Displayed is a 7.55×7.55 cm region of a photo which records 15.1×15.1 cm. The square patterns characteristic of low drive have an rms displacement of 0.17 mm and the turbulent state has an rms amplitude of 1.5 mm.

The diffusing light technique works when the transport mean free path (the distance over which a ray scatters through a large angle) of the light is larger than the surface displacement ζ but smaller than the fluid depth [17]. An important feature of this new method of imaging is that the local surface slope does not affect the amount of light transmitted through a small aperture focused onto the surface. Changes in the solid angle of collected light due to refraction are offset by changes in the surface area subtended by a fixed aperture.

In the absence of polyballs, light propagating through the water will suffer varying amounts of refraction as determined by the local curvature of the surface. The exiting rays form distinctive shadowgraph patterns on a diffusing glass plate located *above* the surface [2,18]. For amplitudes ζ, substantially smaller than those shown in Fig. 1, these rays cross and form caustics and so prevent the deconvolving of ζ from the shadowgraph. The higher the amplitude, the worse is this catastrophe. The advantage of the diffusing light technique is demonstrated by the smoothness of the renditions in Fig. 1 and is also illustrated by Fig. 2 which shows a topographical reconstruction of the instantaneous state of a nonpropagating soliton [19]. The surface slopes (i.e., Mach numbers) in this state range from $+1$ to -1, yet no distortions are apparent; in fact, cross sections taken along the length of the channel accurately match the hyperbolic secant profile characteristic of this high amplitude self-localized motion [20].

Figure 3 displays the power spectrum of the motion as obtained by averaging the Fourier transforms of many photos taken under the same conditions as Fig. 1 (bottom). Note that the harmonic response characteristic of low drive levels transitions to a broadband spectrum at high amplitude. The high amplitude or wave turbulent motion is characterized by a peak at the wave number 6.4 cm^{-1} (which corresponds to the primary parametric response at 25 Hz; half the drive frequency) where energy is injected into the fluid. The energy then cascades to shorter wavelength or higher wave number k where the energy per unit wave number is proportional to a power of "k." This is the inertial region of the turbulent motion. At still higher wave numbers the spectrum merges into the noise. The triangular points in Fig. 3 show the power spectrum contained in a 45° segment of the Fourier transform of a single photo. Since it closely approximates the average, we conclude that the wave turbulence is isotropic. Parametric excitation of waves differs from wind generated waves [21] in that there is no preferred direction.

The power law for the spectrum in the inertial region can be derived in parallel with Kolmogorov's law of vortex turbulence. If E_k denotes the ripple energy per unit area between k and $2k$ then the rate at which nonlinear interactions cause energy to rollover (or cascade) to the range ($2k$,$4k$) is given by

$$\left.\frac{dE_k}{dt}\right|_+ \approx G^2 \omega_k E_k^2/\sigma - 4\mu k^2 E_k \,, \tag{1}$$

where σ is the surface tension and μ is the kinematic viscosity. The nonlinear coefficient of interaction [22] is given by

$$G^2 = 8\pi^4/13\,. \tag{2}$$

For capillary waves the dispersion law bends upward

$$\omega^2 = (\sigma/\rho)k^3, \tag{3}$$

where ρ is the fluid density. According to this so-called decay spectrum two capillary waves can interact to create a third wave. For this reason the lowest order nonlinear term, as in Eq. (1), which describes the change in the spectrum of ripples due to scattering, is quadratic in the

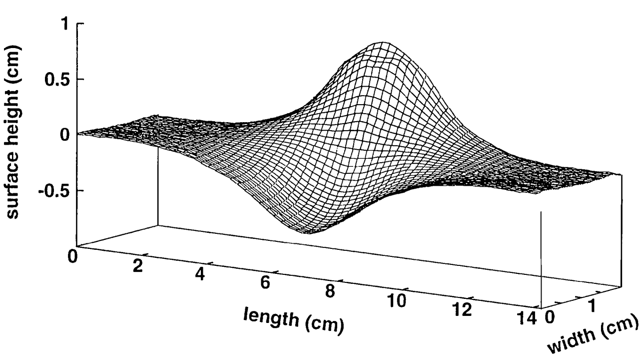

FIG. 2. Perspective of a high amplitude nonpropagating soliton on the surface of water reconstructed from a diffusing light photo. The soliton is localized along the length of the channel. Note the different scales for the length and width of the channel.

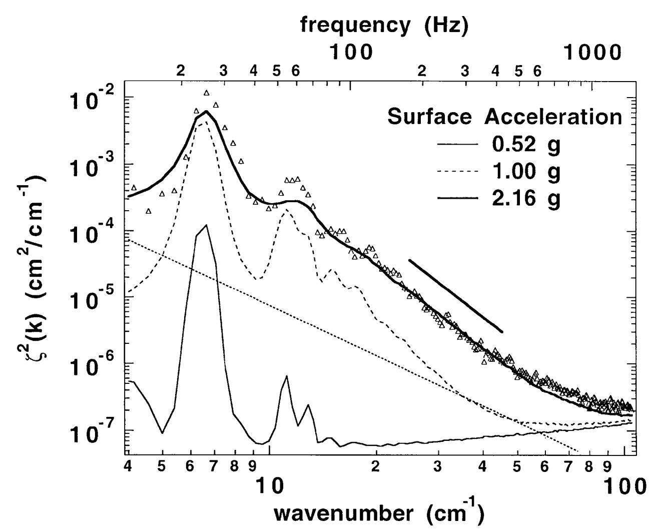

FIG. 3. Spectrum of surface height motion as a function of wave number as obtained from Fourier transforms of Fig. 1. The triangles display the power in a 45° sector of the Fourier transform as obtained from a single photo. The straight line has a slope of -4.2. For reference the frequency as determined by the dispersion law is plotted on the top axis.

energy. In addition to the cascade driven by this nonlinear term, energy can be lost due to linear viscous damping. Turbulence results when the reversible nonlinearities beat out the linear (viscous) damping, or

$$1/\tau_+ \equiv G^2 \omega_k E_k/\sigma \gg 4\mu k^2. \qquad (4)$$

The dashed line in Fig. 3 indicates the threshold which must be exceeded for the turbulent state to be realized. It follows from Eq. (4) when "≫" is replaced with a factor of 10. The motion clearly meets this criterion.

The form of Eq. (1) is dictated by the three ripple interaction, dimensional considerations, and the locality of interactions in k space [7,8]. In a steady state characterized by an energy throughput "q" the energy rollover is independent of k so that when (4) applies:

$$E_k \approx [q\sigma/G^2\omega_k]^{1/2}. \qquad (5)$$

In the continuous limit (5) implies that the spectrum of surface motion obeys

$$\zeta^2(\omega) \approx q^{1/2}\sigma^{1/6}/\rho^{2/3}\omega^{17/6}, \qquad (6)$$

$$\zeta^2(k) \approx q^{1/2}\rho^{1/4}/\sigma^{3/4}k^{15/4}, \qquad (7)$$

where power spectra in k and ω are connected by the relation

$$\int_0^\infty \zeta^2(k)dk = \int_0^\infty \zeta^2(\omega)d\omega = \langle \zeta(\vec{r})^2 \rangle, \qquad (8)$$

where $\langle\,\rangle$ denotes the average value and the total energy density of ripple motion is

$$E = \sigma \int k^2 \zeta^2(k)dk\,. \qquad (9)$$

Turbulent physical systems with energy densities that follow powers of k and ω include vortex motion induced by tides [5], Alfvén waves in the solar wind [23], and surface gravity waves in a stormy sea [24]. Even the distribution of wealth in widely disparate economies follows such a law which was originally referred to as a Pareto distribution [25].

Another criterion for turbulence, which in fact distinguishes it from chaos, is that turbulence involves many modes. That is, there must be many modes activated within the bandwidth due to the nonlinear rollover rate $1/\tau_+(\omega)$. If the number of excited modes per unit frequency is $N(\omega)$ then turbulence occurs when also

$$N(\omega)/\tau_+(\omega) \gg 1\,. \qquad (10)$$

[The density of capillary modes available for excitation is $N_0(\omega) = S\omega^{1/3}/3\pi(\sigma/\rho)^{2/3}$ where S is the surface area.]

An independent measurement of the frequency dependence of the ripple motion was obtained with a photodiode focused onto a 200 μm diameter spot on the surface. Using continuous illumination, data were acquired at a sampling rate of 4 kHz with 16 bits of resolution. The power spectra (again) show that as the amplitude of excitation is increased motion at harmonics of half the drive transition into a broadband turbulent power spectrum [26] that extends for almost one decade in frequency with an exponent (-3.2) that is close to that of Eq. (8). The data indicate that $\zeta^2(\omega)$ is $[d\omega/dk]^{-1}\zeta^2(k)$ as taken from Fig. 3. The similar structure of the spatial k and temporal ω spectra shows that the breadth of the spectrum is due to a large density of excited modes. That is, we are measuring turbulence and not chaos.

Attempts to derive a kinetic equation [7–9,11,12,27] for the nonlinear evolution of normal modes make a number of fundamental assumptions which can now be tested for the turbulent state. These include smoothness of the underlying distribution, retention of the leading order in a multiple time scales expansion, and a Stosszahl ansatz or a lack of statistical correlation between energy in different modes. This cross correlation is defined by

$$\langle \zeta^2(\omega_i)\zeta^2(\omega_j)\rangle / \langle \zeta^2(\omega_i)\rangle \langle \zeta^2(\omega_j)\rangle - 1 = P_{ij}\,, \qquad (11)$$

where $P_{ij} = 0$ for $i \neq j$ when the modes are uncorrelated. Figure 4 shows P_{ij} for $i = 300$ and 25 Hz. The degree of correlation is significant especially the (unexplained) bump in the turbulent regime at around 400 Hz. Whether this peak is due to the excitation of a collective mode of turbulence will be answered by future investigations.

As the amplitude of sinusoidal excitation of water is increased its surface motion, for k and ω, displays a transition to broadband motion characteristic of wave turbulence. Wave-number spectra have been obtained by direct measurement without the need to invoke strong assumptions such as the "Taylor hypothesis" [6]. Although the power spectrum (Fig. 3) defines the turbulent state, the versatility of the new imaging technique enables one to look beyond Fourier decomposition and probe assumptions which underlie various theoretical approaches to turbulence (Fig. 4).

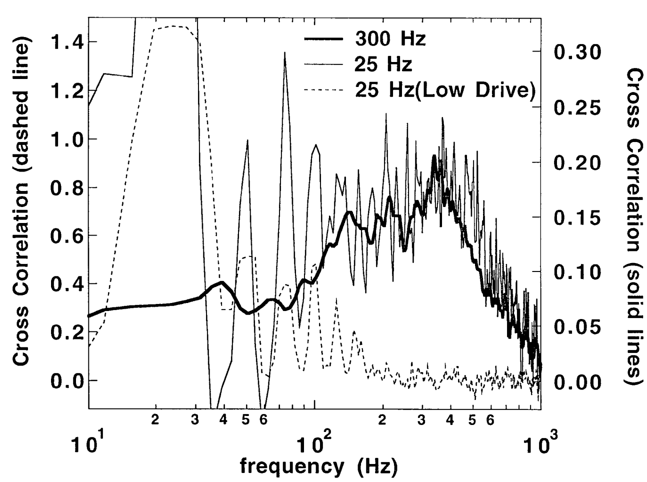

FIG. 4. Cross correlation between motion at different frequencies. The peak in the deviation from the Stosszahl ansatz at 400 Hz in the turbulent state is unexplained. Shown are P_{ij} for, $i = 25$ Hz at low drive and $i = 300$ Hz at high drive. The peaks are structure and not noise.

Future work will aim to search for collective modes in turbulence that are akin to second sound (He^4) [28] or zero sound (He^3) [29], and increase the range of the inertial region (and eliminate the effects of boundaries) by studying ripples on a levitated drop. An exciting challenge is to develop new means of analyzing data (e.g., Fig. 1) to reveal off-equilibrium structures.

This research is supported by the U.S. DOE Division of Engineering and Geophysics and NASA Microgravity Research. Valuable discussions with M. Barmatz, P.H. Roberts, T. Erber, B. Denardo, A. Larraza, R. Hiller, R. Löfstedt, and R. Keolian are gratefully acknowledged. We are especially indebted to Dave Pine for valuable analysis of the imaging technique.

[1] N.B. Tufillaro, R. Ramshankar, and J.P. Gollub, Phys. Rev. Lett. **62**, 422 (1989); A.B. Ezersky, S.V. Kiyashko, P.A. Matusou, and M.I. Rabinovich, Europhys. Lett. **26**, 183 (1994); S.T. Milne, J. Fluid Mech. **225**, 81 (1991); B. Christiansen, P. Alstrom, and M. Levinsen, J. Fluid Mech. **291**, 323 (1995).

[2] B. Christianson, P. Alstrom, and M.T. Levinsen, Phys. Rev. Lett. **68**, 2157 (1992); R. Blümel, I.H. Davidson, W.P. Reinhardt, H. Lin, and M. Sharnoff, Phys. Rev. A **45**, 2641 (1992).

[3] A.N. Kolmogorov, Dokl. Akad. Nauk. SSSR **30**, 301 (1941).

[4] A.M. Oboukhov, Dokl. Akad. Nauk. SSSR **32**, 19 (1941).

[5] H.L. Grant, R.W. Stewart, and A. Moilliet, J. Fluid Mech. **12**, 241 (1962).

[6] S.G. Saddoughi and S.V. Veeravalli, J. Fluid Mech. **268**, 333 (1994).

[7] R.Z. Sagdeev, Rev. Mod. Phys. **51**, 1 (1979).

[8] V.E. Zakharov, V.S. L'vov, and G. Falkovich, *Kolmogorov Spectra of Turbulence* (Springer, Berlin, 1992).

[9] R. Kraichnan, Phys. Fluids **11**, 265 (1968); **9**, 1728 (1966).

[10] V. Yakhot, S.A. Orszag, and Z.S. She, Phys. Fluids **A1**, 184 (1989).

[11] S.J. Putterman and P.H. Roberts, Phys. Rep. **168**, 209 (1988).

[12] A.C. Newell, Rev. Geophys. **6**, 1 (1968).

[13] W. Wright, R. Budak, and S. Putterman, J. Acoust. Soc. Am. **96**, 3322 (1994).

[14] Source: Bangs Laboratories, Carmel, Indiana.

[15] L.D. Landau and E.M. Lifshitz, *Fluid Mechanics* (Pergamon, New York, 1959).

[16] A. Ishimaru, *Wave Propagation and Scattering in Random Media* (Academic, New York, 1978).

[17] Detailed analysis of the technique will be published separately.

[18] B.J. Gluckmen, P. Marq, J. Bridges, and J.P. Gollub, Phys. Rev. Lett. **71**, 2034 (1993); E. Bosch and W. van de Water, Phys. Rev. Lett. **70**, 3420 (1993).

[19] J. Wu, R. Keolian, and I. Rudnick, Phys. Rev. Lett. **52**, 1421 (1984).

[20] A. Larraza and S. Putterman, J. Fluid Mech. **148**, 443 (1984); J. Miles, J. Fluid Mech. **148**, 451 (1984).

[21] G.T. Lleonart and D.R. Blackman, J. Fluid Mech. **97**, 455 (1980).

[22] G.E. Falkovich, I. Ya. Shapiro, and L. Shtilman, Europhys. Lett. **29**, 1–6 (1995); consider a kinetic equation for the evolution of a spectrum of ripples described by the action $n(k)$ where k is the two-dimensional wave number of the surface displacement. This integral equation reduces to the simplified form (1), with nonlinear coefficient approximately given by (2) when the spectrum is isotropic, and the energy and interactions are binned into octaves so that $E_k = 2\pi \int_k^{2k} \omega_k n(k) k dk$. Using the methods of V.E. Zakharov and R.Z. Sagdeev [Sov. Phys. Dokl. **15**, 439 (1970)] it can be shown that the steady state solution [i.e., Eq. (5) below] of (1) and the full kinetic equation agree.

[23] C.T. Russell, in *Solar Wind*, edited by C.P. Sonett, P.J. Coleman, Jr., and J.M. Wilcox (NASA Report No. SP-308 NASA Scientific and Technical Information Office, Washington, DC, 1972).

[24] G.Z. Forristall, J. Geophys. Res. **86**, 8075–8084 (1981).

[25] V. Pareto, *Cours d'Economie Politique* (Rouge, Lausanne, 1896); *Manuale d'Economia Politica* (Societa Editrice Libraria, Milan, 1907) [English Translation: (Augustus M. Kelley, New York, 1971)]; R. Cirillo, *The Economics of V. Pareto* (Frank Cass & Co., London, 1979).

[26] W. Wright, R. Hiller, and S. Putterman, J. Acoust. Soc. Am. **92**, 2360 (1992).

[27] D.J. Benney and P.G. Saffman, Proc. R. Soc. London A **289**, 301 (1966); P. Westervelt, J. Acoust. Soc. Am. **59**, 760 (1976).

[28] A. Larrazza, S.L. Garrett, and S. Putterman, Phys. Rev. A **41**, 3144 (1990).

[29] A. Larraza and G.E. Falkovich, Phys. Rev. B **48**, 9855 (1993).